Advances in Science and Technology Research Journal

Advances in Science and Technology Research Journal 2022, 16(6), 140–146
https://doi.org/10.12913/22998624/156013
ISSN 2299–8624, License CC-BY 4.0

Received: 2022.09.16
Accepted: 2022.11.17
Published: 2022.12.01

Methodological Aspects of Rat Bone Mechanical Impact

Anna Skic[1], Paweł Kołodziej[1*], Iwona Puzio[2], Grzegorz Tymicki[2], Karolina Beer-Lech[1], Krzysztof Gołacki[1]

[1] Department of Mechanical Engineering and Automation, University of Life Sciences in Lublin, ul. Głęboka 28, 20-612 Lublin, Poland

[2] Department of Animal Physiology, Faculty of Veterinary Medicine, University of Life Sciences in Lublin, ul. Akademicka 12, 20-950 Lublin, Poland

* Corresponding author's e-mail: pawel.kolodziej@up.lublin.pl

ABSTRACT

A three-point bending test under quasi-static load conditions is usually used in studies on the bones' mechanical properties. On its basis, the bone strength is determined, corresponding to the maximum force required for the fracture. In natural conditions, bone fractures most often occur as a result of an impact or fall, i.e. under dynamic loads, when a large force acts on the bone in a concise time. This work presents the results of a dynamic two-point bending test of rat bones. Two groups of the humerus were analyzed: healthy (as a control) and ovariectomized rats (as an osteoporosis model). During the bending test in the analyzed bone cross-section, a complex state of the surface density of internal forces will appear, characterized by the simultaneous occurrence of normal and tangential stresses. The obtained results determined the influence of osteoporotic changes on the transmitted dynamic forces values. The values of tensile and compressive stresses occurring at bone fracture were dependent rather on the bone asymmetry, the moment of inertia of its cross-section, and material properties than the loading force.

Keywords: impact loading, pendulum, rat bone, deflection.

INTRODUCTION

Bone is a composite material consisting of organic and inorganic components. Their composition and interaction affect the mechanical properties and strength under different loading conditions [1]. External loads affecting the skeletal system of living organisms cause a complex state of stress inside the bones. After exceeding the permissible values, they lead to cracks, fractures, damages, etc. The action of forces and moments of forces may be different. The most common overloads and related damages are the results of dynamic loads. The way the bone responds to loads is influenced by many factors including porosity, density, mineral content, species, diseases, age, gender, and bone location [1–3]. In particular, the mechanical and geometrical properties of bone indirectly determine its behavior under loading conditions, influencing its performance under stress and strain to provide mechanical stiffness [1]. It is worth noting that the cortical bone shows different mechanical properties than the trabecular. Cortical bone is stiffer in compression under longitudinal loads and under higher strain rates in comparison to trabecular bone. In turn, the porous trabecular bone shows a greater elasticity. Differences in macroscopic composition with dissimilar stress-strain characteristics highlight a complex dependence of applied loads, deformation, and mechanical response of bones [1].

Classic methods of testing the mechanical properties of bones are based on quasi-static analysis. This analysis allows for the description of the sample's response when it is acted on by a single force [4–7] According to the literature data the load direction affects the cortical bone's fracture mechanism and it is related to the osteon's alignment [7]. Higher resistance to fracture was observed for samples with osteons aligned

perpendicularly to the loading direction. This was related to the biaxial stress state caused by bending and shear stress occurrence [6,7]. Trabecular bone as a dynamic, remodeling tissue is consisted of a calcified bone matrix and marrow. The calcified matrix is mechanically viscoelastic [8]. The viscoelasticity of the calcified matrix is related to the collagen matrix, which increases bone plasticity and ductility [9]. Changes in the collagen matrix with age can make the calcified matrix more brittle [8]. In the case of estrogen deficiency condition, imbalance in bone remodeling, in which bone resorption exceeds formation [10].

The examination of fracture under dynamic loading was analyzed in the case of engineering materials, like epoxy resins, polyurethane foam materials aluminum alloy, etc. [11–13]. In the literature describing the mechanical properties of bones, there are few reports characterizing the behavior of bones under impact loading. Prot et al. [14] and Laporte et al [15] analyzed the mechanical properties of cancellous bovine bone samples under dynamic compression, using high strain rates and concluded that the bone response to compression revealed a foam-type behavior over the whole studied range of strain rates. Zhai et al. [16] analyzed the loading rate effect on the fracture toughness of porcine bone specimens and found that the fracture initiation of cortical bone decreased as the loading rate increased. Adharapurapu et al, [17] analyzed the mechanical response of bovine cortical bone samples under varying strain rates. The authors stated that for higher loading rates the bone exhibited lower fracture toughness. Similar results were obtained by Skic et al., [18], who showed that the force needed to fracture under dynamic loads was lower than the force at fracture under quasi-static conditions.

The bone fracture presented in the works [5–7] concerned three-point bending during tests with different loading speeds carried out on samples cut out or on whole bones. This allows for the determination of the mechanical properties described by commonly used material coefficients or indicators (e.g. stress intensity, Young, Kirchhoff, Poisson's ratio) as well as stress or deflection fields. These are the quantities and distributions determined in quasi-static conditions. Different materials with similar strength properties may show substantially different tendencies to fracture under impact loading. Therefore, their static characteristics lose their importance in assessing the ability to withstand this type of load. In order to determine the manner of bone fracture during injuries, mechanical tests simulating the conditions in which these injuries occur should be carried out. This paper presents the results of tests involving the bending of rat humerus with one end fixed and the other free, under dynamic loading conditions. Two bone groups were investigated: the bones of rats induced with osteoporosis and the bones of healthy animals as a control group.

MATERIALS AND METHODS

The research was carried out with the approval of the Local Ethics Committee for animal experiments at the University of Life Sciences in Lublin, Poland (No 23/2015). In the experiment humerus from 8 Wistar rats were used. After acclimatization period (7 days) random rats 3 months aged underwent pseudogonadectomy surgery (CONTROL, n=4) and ovariectomy (OVX, n=4) performed to mimic the postmenopausal osteoporosis process, leading to a low bone mass state. The surgical procedures were carried out under general anesthesia (intramuscular injections were used applying of ketamine (Biowet-Puławy, Poland), atropinum sulphuricum (Polfa-Warsaw, Poland) and xylazine (Biowet-Puławy, Poland) in doses of 3 mg/kg BW, 0.05 mg/kg BW and 10 mg/kg BW, respectively. During experiment the animals were maintained in standard environmental conditions (temperature 22°C ± 2°C, day/night cycle 12h/12h, humidity 55% ± 5%) with constant access to water and feed (LSM, Agropol, Motycz, Poland). After a 20-week period, the animals were euthanized by CO_2 overdose. After euthanasia bones were isolated and stored at -20°C for mechanical analyses.

To prepare the specimen for the test, two-component epoxy glue (Poxipol, Fenedur S.A., Uruguay) was used, that dries after about 10 minutes at 20°C, has no volumetric shrinkage and its strength after hardening in the given time is sufficient to immobilize the bone and conduct the test. The bone embedment depth (*BED*) in the glue-filled PVC tube was set obligatorily at 13 mm, measured from the face of the tube to the axis of the hip joint head (Fig. 1). The test sets prepared in this way were mounted in a clamping fixture connected to a vertical plate forming part of a test stand equipped with a physical pendulum, on

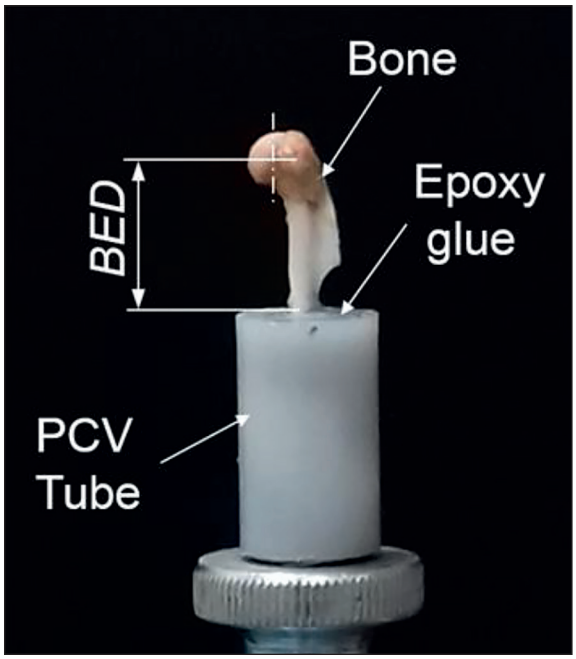

Figure 1. Test kit (TK) for bone impact study with bone embedment depth (BED)

which a force sensor was placed with a flat impactor (Fig. 2).

The device for impact tests (Fig. 2) is constructed from a base with two columns rigidly fixed to the wall and three horizontal connectors. The main plate mounted on the columns can be moved vertically. Additionally, vertical plate that moves horizontally is attached to the main plate and their position can be fixed by adjusting screws. The pendulum arm was mounted on the axis of the incremental angular displacement sensor with an accuracy of 0.005 °(RON 275, Heidenhain, Germany). The arm was fitted with a piezoelectric force sensor (Endevco Corporation, USA) with a sensitivity of 2.27 $mV \cdot N^{-1}$ and a measuring range of ± 220 N. The sensor was connected to the SCB-68 measurement card (National Instruments, USA) transmitting signals to the application worked in LabView ver. 8. 6. 1 environment. It was used to directly measure the angular displacement of the pendulum in time.

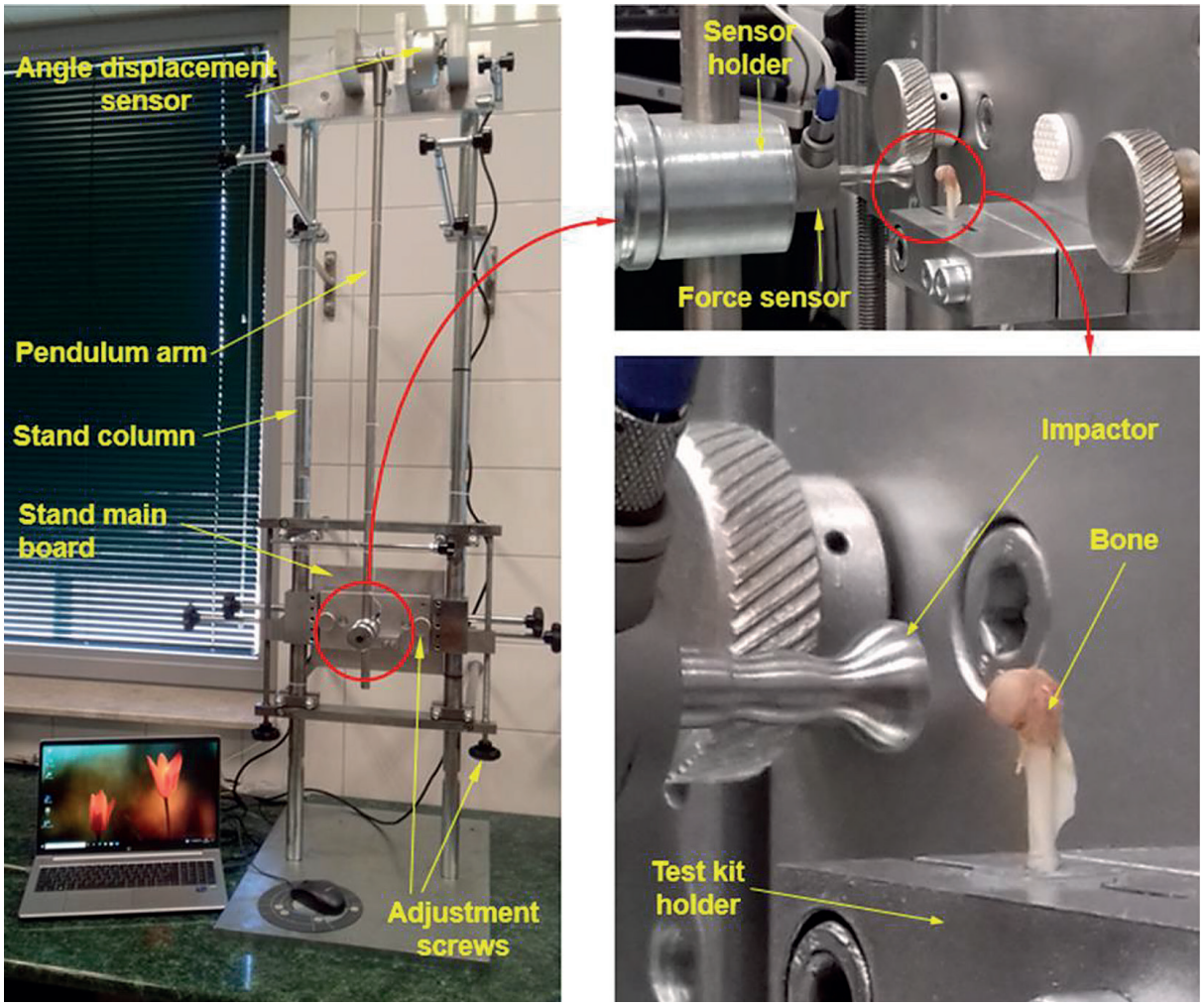

Figure 2. Test stand for dynamic testing of rat bones (description in the text).

The mass moment of inertia of the pendulum arm I_P = 0.072 kg·m^2 allowed to obtain a constant velocity (V_1) during the impact. Before starting the test, the pendulum was set vertically, the angular displacement sensor readings were zeroed, and then the arm was deflected by an angle of 9.15° that allowed to obtain a specific speed value V_1 = 0.5 m·s^{-1} [18–20].

RESULT AND DISCUSSION

Figure 3a shows a scheme of bone loading during impact. *BED* height (13 mm) is the arm of the maximum dynamic loading force (F_{max}). The mathematical product of these two quantities describes the maximum dynamic bending moment M_{DB}:

$$M_{DB} = F_{max} \cdot BED \tag{1}$$

Figure 3b presents a bone cross-section after impact test taken with a stereoscopic microscope (Nikon SMZ18, Nikon Corporation, Tokyo, Japan).

In the tested system, the broken cross-section, located parallel to the direction of force F_{max}, will be loaded simultaneously by the bending moment M_{DB} and the shear force $T_{max} = F_{max}$, which acts along the x axis of inertia. Figure 3b shows a bone cross-section after a mechanic impact. During the bending test in the analysed bone cross-section, a complex state of the surface density of internal forces will appear, characterized by the simultaneous occurrence of normal and tangential stresses. The normal stresses, i.e. bending stresses, can be presented as stretching in the area from point A to the y axis and compression occurring from the y axis to point B. However, tangential stresses, i.e. shear stresses, the value of which will be constant in the cross-sectional plane, are the effect of force T_{max} (Fig. 3). The values of individual stresses were determined from the relationship [21]:

$$\sigma_A = \frac{M_{DB} \cdot e_1}{I_{yC}}; \qquad \sigma_B = \frac{M_{DB} \cdot e_2}{I_{yC}}; \qquad \tau_t = \frac{T_{max}}{A} \tag{2}$$

where: σ_A – maximum tensile stress [MPa],
σ_B – maximum compressive stress [MPa],
τ_t – shear stresses [MPa] (as presented in Fig.4),
e_1, e_2 – distances of points A and B from the neutral y axis [mm],
I_{yC} – the moment of inertia of the cross-section about the neutral axis of bending [mm^4],
A – bone cross-sectional area [mm^2].

To determine the reduced (equivalent) stresses σ_{redA} and σ_{redB}, taking into account the simultaneous occurrence of normal and tangential stresses, the relationship describing the H-M-H (Huber – von Mises – Hencky) hypothesis was used:

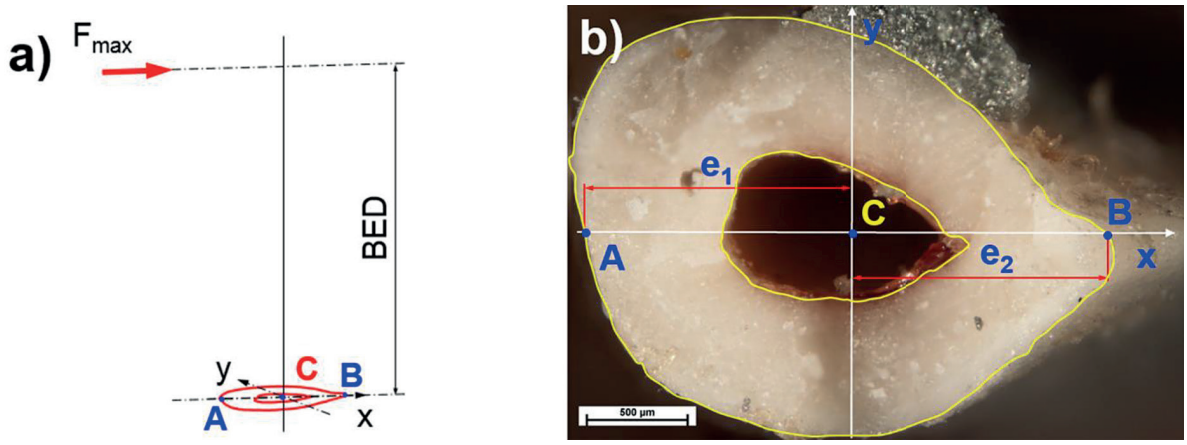

Figure 3. Two-point bone fracture: a) load scheme b) – bone broken cross-section; F_{max} – maximum dynamic load force, *BED* – arm of the maximum dynamic loading force F_{max}, C – center of the cross-section gravity, A – internal and B – external point of the cross-section on the axis of inertia, e_1 and e_2 – distances of points A and B from the neutral y axis of cross-section inertia

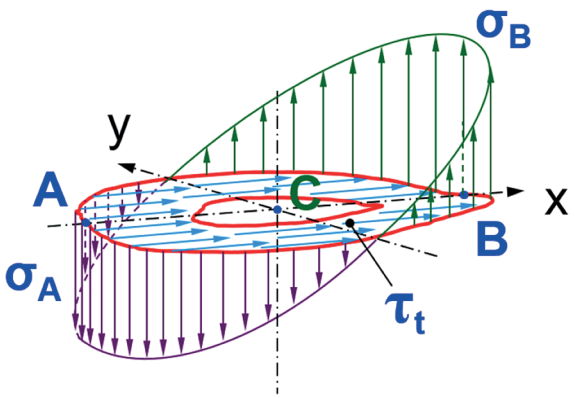

Figure 4. Distribution model and type of stress in the bone cross-section during two-point impact bending.

$$\sigma_{redA} = \sqrt{(\sigma_A)^2 + 3 \cdot \tau_t^2};$$
$$\sigma_{redA} = \sqrt{(\sigma_B)^2 + 3 \cdot \tau_t^2} \quad (3)$$

The courses of the rat bone response in time are presented in Fig. 5. The observed curves are almost linear up to the F_{max} value. Before reaching the maximum value of impact force, a slight bend in curves is observed, which could be related to temporary increase in bone strength just before fracture (strengthening of the material). Bones from the OVX group were characterized by lower F_{max} values and lower slope of the force-time curves. It could be related to cortex thinning and trabecular bone loss as a result of ovariectomy [22, 23].

The results of impact tests of rat's humerus presented in the paper allow for determination of the influence of osteoporotic changes on the transmitted dynamic forces values. The bone characteristic dimensions were determined based on the fracture images. Tables 1 and 2 present the geometrical parameters and results obtained in the performed tests. Higher mean values of calculated stresses were obtained for the CONTROL group, which corresponded to the higher mean value of maximum impact force. For Bone 4 (CONTROL), the highest values of tensile and compressive stresses were obtained (Table 2) in the extreme areas of the bone (points A and B). It is a result of the smallest area of cross-section A (Table 1), the related value of the inertia moment, and also its asymmetry expressed by differences in the lengths of e_1 and e_2. In the OVX group, the highest value of I_{yc} was obtained for Bone 2 which corresponded to the highest geometrical parameters (A, e_1, e_2). For this bone, the lowest values of σ_A, σ_B, and τ_t were obtained (Table 2). The value of bone deflection during impact was determined using the angular displacement recorded by the pendulum arm deflection sensor. Due to its small value, it was considered that the deflection is the length of the rectilinear segment, measured from the beginning of the impactor's contact with the bone head surface to the position corresponding to the maximum force of the mechanical impact. The lower values of bone deflection corresponded to the higher forces and the lower reduced stress (for mean values). The destructive forces for healthy bones (CONTROL) are 17.3% to 57.5%

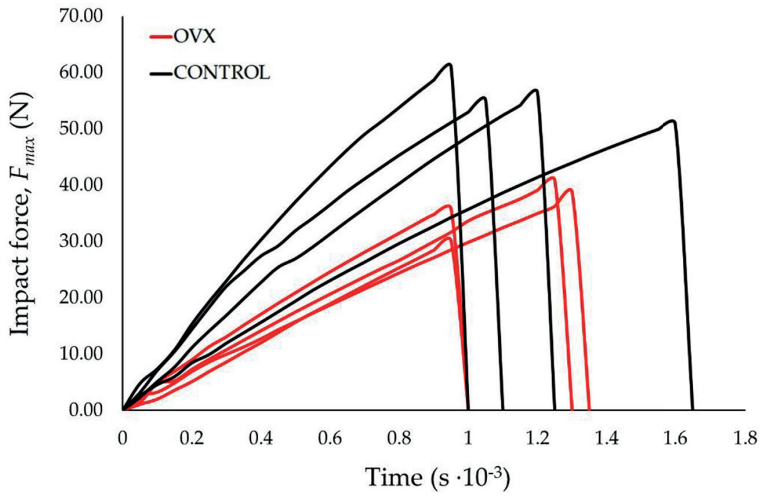

Figure 5. Rat humerus responses during mechanical impact

Table 1. Geometric parameters of analyzed bones

Parameter		Bone length *l* (mm)	Cross-section area *A* (mm^2)	e_1 (mm)	e_2 (mm)	Moment of inertia I_{vc} (mm^4)
CONTROL	Bone 1	29.07	3.318	1.136	1.441	1.5438
	Bone 2	26.65	3.648	1.311	1.396	2.1303
	Bone 3	26.07	3.561	1.247	1.487	1.8903
	Bone 4	26.07	3.016	1.000	1.220	1.1426
OVX	Bone 1	26.13	3.148	0.937	1.324	1.1662
	Bone 2	27.16	4.102	1.543	1.879	3.5760
	Bone 3	26.57	3.795	1.341	2.102	2.9164
	Bone 4	26.13	3.334	1.273	2.051	2.4551

higher than the fracture forces for osteoporotic bones (OVX). While the stress values at the moment of failure in tensile and compressive stresses depend to a lesser extent on the load force but more strongly on the asymmetry and the moment of inertia of the bone cross-section. Tensile stresses were 5.40%÷18.07% lower than compressive stresses for CONTROL, and for OVX bones this range is from 17.88% to 37.01%. Similar findings showed Osterhoff et al. [24], who stated that geometrical measures including bone size, cross-sectional area, or area moment of inertia explain up to 80% of the biomechanical behavior of whole bones. OVX bones showed lower mechanical parameters compared to the CONTROL group. Tangential-shear stress depending on the loading force and cross-sectional area accounts for 2.61% to 3.38% (CONTROL) and 3.03% to 4.43% (OVX) of the reduced normal stresses, and their effect on impact bone fracture was minimal. Our results are consistent with those obtained by Xi et al. [25] who found that the mechanical competence of osteoporotic bones was reduced in the compression and tension test. As observed by other authors, [26] an increase in bone fragility after rats' ovariectomy can be related to the deterioration of the material properties and geometric changes resulting from an imbalance between bone formation and resorption.

CONCLUSIONS

A destructive and dynamic two-point bending test was developed and performed to analyze the bone reaction in time on the external impactor load. The adopted sample fixing and loading method allow for obtaining a bone response to impact until fracture. Tests confirmed differences in the maximum values of fracture forces and normal tensile stresses for healthy (CONTROL) and osteoporotic (OVX) bones. Lower bone deflection values corresponded to higher force values that showed the dynamic nature of the test. However, the work did not explain the failure criterion in two–points dynamic bone bending. The tensile and compressive stress values occurring at the moment of failure depend to a lesser extent on the load force but higher on the bone asymmetry and the moment of inertia of its cross-section. The dynamic fracture occurs at dominant normal stresses for which tensile stresses are lower than compressive (depending on the asymmetry of the bone cross-section). Tangential-shear stress that depends on the loading force and cross-sectional area had a minimal effect on bone fracture.

Table 2. Values of maximum impact forces, bone deflection, and stresses obtained in two-point bending test

Parameter		Impact force F_{max} (N)	Bone deflection (mm)	Max. Tensile stress σ_A (MPa)	Max. Compression stress σ_B (MPa)	Shear stress τ_t (MPa)	H-M-H stress σ_{redA} (MPa)	H-M-H stress σ_{redB} (MPa)
CONTROL	Bone 1	50.89	1.396	584.33	617.73	15.27	584.90	618.29
	Bone 2	60.97	1.090	488.02	519.43	16.56	488.86	520.22
	Bone 3	58.41	1.064	501.23	597.35	16.40	502.03	598.03
	Bone 4	56.14	1.308	638.69	779.65	18.61	639.50	780.31
OVX	Bone 1	38.72	1.884	404.71	571.75	12.29	405.27	572.15
	Bone 2	42.08	1.361	236.05	287.48	10.46	236.74	288.06
	Bone 3	41.61	1.823	248.87	389.96	10.96	249.59	390.42
	Bone 4	40.81	1.073	275.19	443.24	12.24	276.00	443.74

REFERENCES

1. Hart N.H., Nimphius S., Rantalainen T., Ireland A., Siafarikas A., Newton R.U. Mechanical basis of bone strength: influence of bone material, bone structure and muscle action. Journal of Musculoskeletal and Neuronal Interactions 2017; 17(3): 114–139.
2. Chittibabu V., Rao S.K., Rao G.P. Factors Affecting The Mechanical Properties Of Compact Bone And Miniature Specimen Test Techniques: A Review. Advances in Science and Technology Research Journal 2016; 10(32): 169–183.
3. Cole J.H., van der Meulen M.C. Whole bone mechanics and bone quality. Clinical Orthopaedics and Related Research 2011; 469(8): 2139–2149.
4. Li S., Abdel-Wahab A., Silberschmidt V.V. Analysis of fracture processes in cortical bone tissue. Engineering Fracture Mechanics 2013; 110: 448–458.
5. Chen Y., Yang D., Ma Y., Tan X., Shi Z., Li T., Si H. Experimental investigation on the mechanical behavior of bovine bone using digital image correlation technique. Applied Bionics and Biomechanics 2015: 609132.
6. Aliha M.R.M., Ghazi H., Ataei F. Experimental fracture resistance study for cracked bovine femur bone samples. Frattura ed Integrità Strutturale 2019; 50: 602–612.
7. Carpinteri A., Berto F., Fortese G., Ronchei C., Scorza D., Vantadori S. Modified two-parameter fracture model for bone. Engineering Fracture Mechanics 2017; 174: 44–53.
8. Ojanen X., Isaksson H., Töyräs J., Turunen M.J., Malo M.K.H., Halvari A., Jurvelin J.S. Relationships between tissue composition and viscoelastic properties in human trabecular bone. Journal of Biomechanics 2015; 48: 269–275.
9. Saito M., Marumo K. Collagen cross-links as a determinant of bone quality: a possible explanation for bone fragility in aging, osteoporosis, and diabetes mellitus. Osteoporosis International 2010; 21: 195–214.
10. Chen X., Moriyama Y., Takemura Y., Rokuta M., Ayukawa Y. Influence of osteoporosis and mechanical loading on bone around osseointegrated dental implants: A rodent study. Journal of the Mechanical Behavior of Biomedical Materials 2021; 123:104771.
11. Marsavina L. and Sadowski T. Dynamic fracture toughness of polyurethane foam. Polymer Testing 2008; 27(8): 941–944.
12. Skoczylas J., Samborski S., Kłonica M. Experimental Study on Static and Dynamic Fracture Toughness of Cured Epoxy Resins. Advances in Science and Technology. Research Journal 2019; 13(1): 122–127.
13. Godzimirski J., Komorek Z., Komorek A. An Energy Analysis of Impact Strength Tests Using Pendulum Hammers. Advances in Science and Technology. Research Journal. 2019; 13(4): 214–222.
14. Prot M., Saletti D., Pattofatto S., Bousson V., Laporte S. Links between mechanical behavior of cancellous bone and its microstructural properties under dynamic loading, Journal of Biomechanics 2015; 48(3): 498–503.
15. Laporte S., David F., Bousson V., Pattofatto S. Dynamic behavior and microstructural properties of cancellous bone. In: Proceedings of the DYMAT, Brussels, Belgium 2009, 895–900.
16. Zhai X., Gao J., Nie Y., Guo Z., Kedir N., Claus B., Sun T., Fezzaa K., Xiao X., Chen W.W. Real-time visualization of dynamic fractures in porcine bones and the loading-rate effect on their fracture toughness. Journal of the Mechanics and Physics of Solids 2019; 131: 358–371.
17. Adharapurapu R. R., Jiang, F., Vecchio, K. S. Dynamic fracture of bovine bone. Materials Science and Engineering: C 2006; 26(8): 1325–1332.
18. Skic A., Puzio I., Tymicki G., Kołodziej P., Pawłowska-Olszewska M., Skic K., Beer-Lech K., Bieńko M., Gołacki K. Effect of Nesfatin-1 on Rat Humerus Mechanical Properties under Quasi-Static and Impact Loading Conditions. Materials 2022; 15: 333.
19. Gołacki K., Kołodziej P. Impact testing of biological material on the example of apple tissue. TEKA Kom. Mot. i Energ. Roln. OL PAN 2011; 11c: 74–82.
20. Kołodziej P., Gołacki K., Stropek S., Boryga M., Gładyszewska B., Studies on thermpolastic starch film properties under impact load conditions. Przemysł Chemiczny 2014; 93: 1375–1378.
21. Dyląg Z., Jakubowicz A., Orłoś Z. Wytrzymałość Materiałów. T. 1, WNT Warszawa, 2012.
22. Jiang S.D., Shen C., Jiang L.S., Dai L.Y. Differences of bone mass and bone structure in osteopenic rat models caused by spinal cord injury and ovariectomy. Osteoporosis International 2007; 18(6): 743–50.
23. Gomes R. M., Junior M., Francisco F. A., Moreira V. M., de Almeida D. L., Saavedra L., de Oliveira J. C., da Silva Franco C. C., Pedrino G. R., de Freitas Mathias P. C., Natali M., Dias M. J., de Morais I. J., de Moraes S. Strength training reverses ovariectomy-induced bone loss and improve metabolic parameters in female Wistar rats. Life Sciences 2018; 213: 134–141.
24. Osterhoff G., Morgan E.F., Shefelbine S.J, Karim L., McNamara L.M., Augat P. Bone mechanical properties and changes with osteoporosis. Injury 2016; 47(2): 11–20.
25. Xi L., Wen W., Wu W., Qu Z., Tao R., Karunaratne A., Liao B., Li Y., Fang D. Mechanical response of cortical bone in compression and tension at the mineralized fibrillar level in steroid induced osteoporosis. Composites Part B-engineering 2020; 196: 108138.
26. Popović T., Šrbić R., Matavulj M., Obradović Z., Sibinčić S., Experimental model of osteoporosis on 14 week old ovari-ectomised rats: a biochemical, histological and biomechanical study. Biologia Serbica 2016; 38(1): 18–27.